

Submesoscale streamers exchange water on the north wall of the Gulf Stream

Jody M. Klymak¹, R. Kipp Shearman², Jonathan Gula³, Craig M. Lee⁴, Eric A. D'Asaro⁴, Leif N. Thomas⁵, Ramsey Harcourt⁴, Andrey Shcherbina⁴, Miles A. Sundermeyer⁶, Jeroen Molemaker⁷, and James C. McWilliams⁷

¹University of Victoria, Victoria, British Columbia, Canada

²Oregon State University, Corvallis, Oregon, USA

³Laboratoire de Physique des Océans, Université de Bretagne Occidentale, Brest, France

⁴Applied Physics Laboratory, University of Washington, Seattle,
Washington USA

⁵Stanford University, Stanford, California, USA

⁶University of Massachusetts Dartmouth, Dartmouth,
Massachusetts, USA

⁷University of California, Los Angeles, California, USA

October 7, 2015

18 University of Victoria, Victoria, British Columbia, Canada Oregon State
19 University, Corvallis, Oregon, USA Laboratoire de Physique des Océans, Université
20 de Bretagne Occidentale, Brest, France Applied Physics Laboratory, University
21 of Washington, Seattle, Washington USA Stanford University, Stanford, California,
22 USA University of Massachusetts Dartmouth, Dartmouth, Massachusetts, USA
23 University of California, Los Angeles, California, USA

Abstract

The Gulf Stream is a major conduit of warm surface water from the tropics to the subpolar North Atlantic. Its north side has a strong temperature and salinity front that is less than 5 km wide and is maintained for hundreds of kilometers despite considerable energy available for mixing. Large mesoscale (> 20 km) “rings” often pinch off, but like the Gulf Stream they are resistant to lateral mixing, and retain their properties for a long time. Here we observe and simulate a sub-mesoscale (< 20 km) mechanism by which the Gulf Stream exchanges water with the cold subpolar water to the north. The front exhibits a strong temperature-salinity

34 contrast, with a distinct mode of “mixed” water between the two water
35 masses that is between 2 and 4 km wide. This mass of water is not seen to
36 increase downstream despite there being substantial energy available for
37 mixing. A series of “streamers” detrain some of this water from the Gulf
38 Stream at the crest of meanders. Subpolar water is entrained replacing
39 the mixed water, and helping to resharpen the front. The water mass
40 exchange can account for a northwards flux of salt of $0.8 - 5 \text{ psu m}^2\text{s}^{-1}$,
41 which can be cast as an effective local diffusivity of $O(100 \text{ m}^2\text{s}^{-1})$. This
42 is similar to bulk-scale flux estimates of $1.2 \text{ psu m}^2\text{s}^{-1}$ and is enough to
43 ~~supply supplies~~ fresh water to the Gulf Stream ~~as~~ required for the pro-
44 duction of 18-degree subtropical mode water.

45 The Gulf Stream (GS) is the western boundary current of the North At-
46 lantic subtropical wind-driven circulation. It separates from Cape Hatteras and
47 ~~extends into the interior North Atlantic, traveling east where it flows eastward~~
48 into the North Atlantic. As it does so ~~flows~~, it loses heat not only to the at-
49 mosphere , but also ~~and~~ by mixing with the cold water in the subpolar gyre to
50 the north. It also becomes fresher, an observation that can only be explained
51 by entrainment of fresh water from the north [1]. As it entrains water, the GS
52 increases its eastward transport by approximately $4 - 8 \times 10^6 \text{ m}^3\text{s}^{-1}/100 \text{ km}$
53 (Johns et. al.[2]).

54 The GS has a sharp density front, but it also has a sharp temperature and
55 salinity front, as has been demonstrated at the surface from shipboard surveys[3]
56 and satellite images[4]. The sharpness of the front beneath the surface has
57 been less-clear, and requires high-resolution lateral sampling to resolve. It is
58 also known that the front has a sharp potential vorticity gradient[5], and such
59 gradients act as a barrier to lateral mixing[6, 7]. Despite this barrier, property
60 budgets indicate that there is significant exchange across the north wall[1], and
61 that entrainment of fresh water is necessary to create the dynamically important
62 “18-degree water” that fills much of the upper Sargasso Sea.

63 The mechanisms controlling this lateral mixing have not been identified.
64 There are large eddies that periodically pinch off the GS and carry warm water
65 to the north. However, some of these are re-entrained into the GS and do not
66 result in a net exchange. Instead, tracer budgets across the front appear to be
67 dominated by small-scale processes[8]. To date some of the best direct evidence
68 for cross-front exchange consists of the trajectories of density-following floats
69 placed at the north wall [9, 10]. These floats were observed to regularly detrain
70 from the GS, such that of 95 floats, 26 stayed in the GS, 7 were detrained in
71 rings, and 62 were detrained by mechanisms other than rings[10]. Kinematic
72 theories have been examined to explain the detrainment of the floats [11, 12, 13],
73 and the similarity of the float detrainment to satellite images of “streamers” of
74 warm water detraining from the Gulf Stream ~~have has~~ been noted. However,
75 direct observations of the processes as it occurs at depth have been lacking.

76 Here we present indirect evidence that there is small-scale mixing ($<0.5 \text{ km}$)
77 on the northern cyclonic side of the GS, and that the mixed water periodically
78 peels off the GS in thin (5-10 km wide) “streamers”. In March 2012 we made
79 high-resolution measurements of the north wall of the GS from 66 W to 60 W

(Fig. 1), about 850 km east of where the GS separates from the North American continental slope. Two research vessels tracked a water-following float placed in the GS front and programmed to follow the density of the surface mixed layer. The float was transported downstream with a speed of $1.4 \pm 0.2 \text{ m s}^{-1}$, in water that became denser as the surface of the GS cooled. One vessel maintained tight sampling around the float and deployed an undulating profiler to 200 m, making 10-km cross sections every 10 km downstream. The second vessel had an undulating profiler making larger 30-km scale sections. Both profilers measured temperature, salinity and pressure, and had approximately 1-km along-track resolution; both ships also measured ocean currents. Fluorescent dye was deployed near the floats on some deployments, and measured by the profilers on the ships. By following the float, a focus on the front was maintained as it curved and meandered to the east.

During these observations, the GS had a shallow meander crest at 65 W (Fig. 1b) followed by a long concave region (63 W) and then another large crest (61 W). Satellite measurements show the sharp temperature changes across the front, superimposed with thin intermediate-temperature (15-18°C) streamers detrainning to the north at approximately 65 W, 64 W, and at the crest of the large meander at 61 W. An older streamer that has rolled up can also be seen at 62 W. The ships passed through the three newer streamers providing the first detailed observations of their underwater structure.

The front consists of density surfaces that slope up towards the north (Fig. 2a-d). The water along density surfaces is saltier (and warmer) in the GS, and fresher (and colder) to the north. The transition between the two water masses is remarkably abrupt, occurring over less than 5-km. This sharpness persisted from our western-most section during the cruise (71.5 W) to the eastern-most (60.5 W). Some cross sections clearly show lateral interleaving of salinity north of the front (Fig. 2a) with approximately 5-km wide salinity anomalies ($S \approx 36.15 \text{ psu}$). These anomalies move slower than the front (Fig. 2e), and have high potential vorticity that is normally associated with the front (Fig. 2i).

The temperature-salinity (T/S) relationship of this data shows the contrast between the GS and the subpolar water as two distinct modes (Fig. 3a), except near the surface where the water masses are strongly affected by the atmosphere. For the deeper water, there is a third distinct population between the two larger modes in T/S space that represents the water in the salinity anomalies, and we have labelled as “streamers”. The distinctness in T/S space of the streamers indicates that after the GS and subpolar waters mixed, the partially mixed water continued to mix, condensing it in T/S space (perfectly mixed water would be a dot).

Looking at the GS in plan view (Fig. 3b) we see the mixed water that makes up the streamers is connected along the length of our observations. The first streamer (64.5 W) is horizontally connected over 100 km, and is about 5 km wide, and at least 150 m deep. Where the streamer is the most detached (Fig. 2a) the main front is the sharpest of the 4 cross sections. Downstream of this streamer, the mixed water thins before the eastern meander (60.5 W) where there is a second streamer. Further downstream, the mixed water almost

126 disappears by the last cross-section (59 W). ~~There is a hint of a streamer north~~
127 ~~of the front here, but our section did not go far enough north to define it, but~~
128 ~~the thinning of the front is strong evidence that water has been removed in a~~
129 ~~streamer.~~

130 We can quantify the rate of detrainment from the first streamer (64.5 W). It
131 starts on the fast side of the front with water flowing approximately 0.25 m s^{-1}
132 faster than the float (Fig. 2h). Upstream, where it is detached (Fig. 2e), it is
133 flowing almost 0.5 m s^{-1} slower than the float. A 5-km wide and 150-m deep
134 streamer, with a relative velocity of 0.75 m s^{-1} represents a rate of detrainment
135 of over $0.5 \times 10^6 \text{ m}^3 \text{s}^{-1}$.

136 Concurrently, there is a bolus of fresh water from the north that is enfolded
137 between the streamers and the GS, which we will call an “intrusion”. The
138 entrainment of the intrusion is hard to quantify using the data presented above,
139 because it is drawn from a large pool of water upstream. However, a subsequent
140 survey of the north wall (March 14) included a dye release in this water that
141 was ~~then observed to be~~ entrained in an intrusion (Fig. 4a-c). The streamer
142 during this occupation was less pronounced than the one described above, but
143 was clear for a number of passes through the north wall. The dye cloud was
144 quite spread out, but the data show clear interleaving of the intrusion water.

145 High-resolution numerical simulations ($dx \approx 500\text{m}$, see Methods) resolve
146 these features and also confirm the entrainment of the fresh intrusion (Fig. 4d-
147 i). Seeding the simulation with Lagrangian particles (see methods) allows us to
148 track the evolution of the streamers and the intrusion as the flow moves down-
149 stream. Before the streamer is formed, the water in the intrusion (magenta
150 contours) is near the surface and the streamer water (green contours) is well
151 within the front (Fig. 4d,g). Downstream (Fig. 4e,h) the fresh water has been
152 subducted to 150 m depth, and the streamer has been pushed north of the front.
153 Both water masses accelerate with the GS (Fig. 4f), but the fresh intrusion ac-
154 celerates more, such that the intrusion is entrained and the streamer slows and is
155 detrained. As in the observations, the streamer occupies an intermediate region
156 in T-S space (Fig. 4i, green contour), and originates in the high-vorticity region
157 of the front. The acceleration of the fresh intrusion relative to the streamer is
158 an important finding of the model, as the fresh water now forms a new sharp
159 T-S front with the warm salty GS, and the mixed streamer water is carried away
160 from the front. The model further shows that the streamers are more prominent
161 on the leading edges of meanders, also clearly seen in satellite images (Fig. 1).

162 There are two major implications of the loss of mixed water to the north. The
163 first is that it helps explain why the front at the north wall of the GS remains
164 so sharp. The T/S distribution clearly indicate that there is mixing because of
165 the separate water-class mode. However we also show that the mixing product
166 is carried away in the streamers. It is striking that it is only the mixed water
167 that is carried away, and not high-salinity GS water (Fig. 3b)~~and that this~~
168 ~~is also high-vorticity water.~~ This implies a dynamical link that we have not
169 seen explored. Streamers have been observed in surface temperature satellite
170 images and indirectly by subsurface floats[9, 11, 14, 15], and this has led to
171 kinematic models in which particles are displaced from streamlines going around

propagating meanders [16, 13, 14]. The observations here add to these models by showing that it is only mixed water that leaves the GS. This co-incidence indicates to us a role for small-scale mixing in producing the destabilizing forces that cause this water to detrain from the north wall. The observations and simulation indicate that the meanders of the GS play an important role in the formation of the streamers.

The second implication is that the streamers are a mechanism that can balance large-scale budgets that require significant exchange across the GS[1, 8]. Such budgets suggest that this region of the GS loses salinity to the north at a rate of $1.2 \text{ psu m}^2\text{s}^{-1}$ [1]. Each streamer transports $0.2\text{--}0.5 \times 10^6 \text{ m}^3\text{s}^{-1}$ of water that is $0.8\text{--}1 \text{ psu}$ saltier than the water that is entrained. Streamers appear approximately every 100–300 km, associated with meanders, so an estimate of their average transport is $0.8\text{--}5 \text{ psu m}^2\text{s}^{-1}$, bracketing the large-scale estimates. Working against a gradient of $1 \text{ psu}/10 \text{ km}$ over 200 m depth, the equivalent lateral diffusivity is $40\text{--}250 \text{ m}^2\text{s}^{-1}$. ~~More observations would need to be made to make this transport estimate more robust.~~

Here we have observed a submesoscale lateral stirring process along the north wall of the GS. The T/S front remains persistently sharp, despite small-scale mixing evident from the T/S diagrams, and due to a number of possible processes[17, 18]. The mixed water mass does not accumulate, or it would weaken the sharpness of the front. Here we show that the streamers detrain ~~the~~ mixed water, and entrain cold and fresh water toward the north wall, resharpening the temperature-salinity front. Further analysis of the data and models will shed light on the exact mechanism triggering the ejection of water from the front via the streamers.

1 Methods

The Lagrangian float[19] was placed in the Gulf Stream front based on a brief cross-stream survey, and programmed to match the density of the surface mixed layer (upper 30 m). The float moved downstream at a mean speed of 1.4 m s^{-1} . The *R/V Knorr* tracked the float and deployed a Chelsea Instruments TriAxus that collected temperature, salinity, and pressure (CTD) on a 200-m deep sawtooth with approximately 1-km lateral spacing in a 10-km box-shaped pattern relative to the float (Fig. 1, magenta). *R/V Atlantis* ~~maintained a larger set of performed larger~~ cross sections approximately 30 km across the front, trying to intercept the float on each front crossing. *R/V Atlantis* was deploying a Rolls Royce Marine Moving Vessel Profiler equipped with a CTD that profiled to 200 m approximately every 1 km. Both ships had a 300 kHz RDI Acoustic Doppler Current Profiler (ADCP) collecting currents on 2-m vertical scale averaged every 5 minutes (approximately 1 km lateral scale), collected and processed using UHDAS and CODAS (<http://currents.soest.hawaii.edu>[20]). This data reached about 130 m, and was supplemented at deeper depths with data from 75 kHz RDI ADCPs, with 8-m vertical resolution.

Data were interpolated onto depth surfaces by creating a two-dimensional

215 interpolation onto a grid via Delauney triangulation. No extrapolation was
216 performed. Data on the 26.25 kg m^{-3} isopycnal were assembled at each grid
217 point by finding the first occurrence of that isopycnal in depth.

218 Potential vorticity is calculated from the three-dimensional grid as

$$q = -\frac{g}{\rho_0} (\nabla \times \mathbf{u} + \mathbf{f}) \cdot \nabla \rho, \quad (1)$$

219 where f is the Coriolis frequency, g the gravitational acceleration. The bracketed term is twice the angular velocity, including the planet's rotation, and the
220 gradient of density represents the stretching or compression of the water column.
221 In the GS, the potential vorticity is dominated by contributions from
222 the vertical density gradient and the cross-stream gradient of the along-stream
223 velocity:

$$q \approx N^2 \left(-\frac{\partial u}{\partial y} + f \right). \quad (2)$$

225 Dye Release. At select times during the float evolutions, fluorescein dye
226 releases (100 kg per release) were conducted at depth as close as possible to
227 the float. Dye was pumped down a ~~garden~~-hose to a tow package deployed off
228 the side of the ship, consisting of a CTD and a dye diffuser. Prior to injection,
229 the dye was mixed with alcohol and ambient sea water to bring it to within
230 0.001 kg m^{-3} of the float's target density. Initial dimensions of the dye streak
231 were $\approx 1 \text{ km}$ along-stream, $\approx 100 \text{ m}$ cross-stream (after wake adjustment), and
232 ranging from 1 - 5 m in the vertical. The TriAxis system on the *R/V Knorr*
233 tracked the fluorescein from its CTD package.

234 Numerical simulation. The high-resolution realistic simulation of the GS
235 is performed with the Regional Oceanic Modeling System (ROMS[21]). This
236 simulation has a horizontal resolution of 500m and 50 vertical levels. The model
237 domain spans 1,000 km by 800 km and covers a region of the GS downstream
238 from its separation from the U.S. continental slope. Boundary conditions are
239 supplied by a sequence of two lower-resolution simulations that span the entire
240 GS region and the Atlantic basin, respectively. The simulation is forced by
241 daily winds and diurnally modulated surface fluxes. The modelling approach is
242 described in detail in Gula et. al[22].

243 Virtual Lagrangian Particles. ~~The neutrally~~ Neutrally buoyant Lagrangian
244 (flow-following) particles were seeded at time 285 and advected both backwards
245 and forwards from this time by the model velocity fields without additional
246 dispersion from the model's mixing processes[23]. A 4th-order Runge-Kutta
247 method with a time step $dt = 1 \text{ s}$ is used to compute particle advection. Velocity
248 and tracer fields are interpolated at the positions of the particles using cubic
249 spline interpolation in both the horizontal and vertical directions. We use hourly
250 outputs from the simulation to get sufficiently frequent and temporally-smooth
251 velocity sampling for accurate parcel advection.

252 References

- 253 [1] Joyce, T. M., Thomas, L. N., Dewar, W. K. & Girton, J. B. Eighteen
254 degree water formation within the Gulf Stream during CLIMODE. *Deep*
255 *Sea Res. II* (2013).
- 256 [2] Johns, W., Shay, T., Bane, J. & Watts, D. Gulf stream structure, transport,
257 and recirculation near 68°W. *J. Geophys. Res.* **100**, 817–817 (1995).
- 258 [3] Ford, W., Longard, J. & Banks, R. On the nature, occurrence and origin
259 of cold low salinity water along the edge of the Gulf Stream. *J. Mar. Res.*
260 **11**, 281–293 (1952).
- 261 [4] Churchill, J. H., Cornillon, P. C. & Hamilton, P. Velocity
262 and hydrographic structure of subsurface shelf water at the
263 Gulf Stream's edge. *J. Geophys. Res.* **94**, 10791–10800 (1989).
264 <http://dx.doi.org/10.1029/JC094iC08p10791>.
- 265 [5] Rajamony, J., Hebert, D. & Rossby, T. The cross-stream potential vorticity
266 front and its role in meander-induced exchange in the gulf stream. *J. Phys.*
267 *Oceanogr.* **31**, 3551–3568 (2001).
- 268 [6] Marshall, J., Shuckburgh, E., Jones, H. & Hill, C. Estimates and implica-
269 tions of surface eddy diffusivity in the Southern Ocean derived from tracer
270 transport. *J. Phys. Oceanogr.* **36**, 1806–1821 (2006).
- 271 [7] Naveira Garabato, A. C., Ferrari, R. & Polzin, K. L. Eddy stirring in the
272 southern ocean. *J. Geophys. Res.* **116** (2011).
- 273 [8] Bower, A. S., Rossby, H. T. & Lillibridge, J. L. The Gulf Stream-barrier
274 or blender? *J. Phys. Oceanogr.* **15**, 24–32 (1985).
- 275 [9] Bower, A. & Rossby, T. Evidence of cross-frontal exchange processes in the
276 Gulf Stream based on isopycnal rafos float data. *J. Phys. Oceanogr.* **19**,
277 1177–1190 (1989).
- 278 [10] Bower, A. S. & Lozier, M. S. A closer look at particle exchange in the Gulf
279 Stream. *J. Phys. Oceanogr.* **24**, 1399–1418 (1994).
- 280 [11] Flierl, G., Malanotte-Rizzoli, P. & Zabusky, N. Nonlinear waves and co-
281 herent vortex structures in barotropic β -plane jets. *J. Phys. Oceanogr.* **17**,
282 1408–1438 (1987).
- 283 [12] Stern, M. E. Lateral wave breaking and “shingle” formation in large-scale
284 shear flow. *J. Phys. Oceanogr.* **15**, 1274–1283 (1985).
- 285 [13] Pratt, L. J., Susan Lozier, M. & Beliakova, N. Parcel trajectories in quasi-
286 geostrophic jets: Neutral modes. *J. Phys. Oceanogr.* **25**, 1451–1466 (1995).

- 288 [14] Lozier, M., Pratt, L., Rogerson, A. & Miller, P. Exchange geometry re-
 289 vealed by float trajectories in the Gulf Stream. *J. Phys. Oceanogr.* **27**,
 290 2327–2341 (1997).
- 291 [15] Song, T., Rossby, T. & Carter, E. Lagrangian studies of fluid exchange
 292 between the Gulf Stream and surrounding waters. *J. Phys. Oceanogr.* **25**,
 293 46–63 (1995).
- 294 [16] Bower, A. S. A simple kinematic mechanism for mixing fluid parcels across
 295 a meandering jet. *J. Phys. Oceanogr.* **21**, 173–180 (1991).
- 296 [17] Thomas, L. N. & Shakespeare, C. A new mechanism for mode water for-
 297 mation involving cabbeling and frontogenetic strain at thermohaline fronts.
 298 In press *J. Phys. Oceanogr.*
- 299 [18] Whitt, D. B. & Thomas, L. N. Near-inertial waves in strongly baroclinic
 300 currents. *J. Phys. Oceanogr.* **43**, 706–725 (2013).
- 301 [19] D’Asaro, E. A. Performance of autonomous lagrangian floats. *J. Atmos.*
 302 *Ocean. Tech.* **20**, 896–911 (2003).
- 303 [20] Firing, E., Hummon, J. M. & Chereskin, T. K. Improving the quality
 304 and accessibility of current profile measurements in the southern ocean.
 305 *Oceanography* (2012).
- 306 [21] Shchepetkin, A. & McWilliams, J. The regional oceanic modeling sys-
 307 tem (ROMS): a split-explicit, free-surface, topography-following-coordinate
 308 oceanic model. *Ocean Modell.* **9**, 347–404 (2005).
- 309 [22] Gula, J., Molemaker, M. J. & McWilliams, J. C. Gulf stream dynamics
 310 along the southeastern us seaboard. *J. Phys. Oceanogr.* **45**, 690–715 (2015).
- 311
- 312 [23] Gula, J., Molemaker, M. J. & McWilliams, J. C. Submesoscale cold fila-
 313 ments in the gulf stream. *J. Phys. Oceanogr.* **44**, 2617–2643 (2014).

314 List of Figures

- 1 **Experimental design.** Inset: The experiment site on the north
 315 wall of the Gulf Stream, between 66 and 60 W, as shown in an
 316 AVHRR satellite image of sea surface temperature (SST). Main:
 317 Detailed SST image composed from two ~~satellites~~ satellite im-
 318 ages. The GS is warm and delineated by a sharp front. ~~There~~
 319 ~~are~~The small sub-mesoscale structures north of the front, ~~which~~
 320 are the focus of this paper. The satellite images are a com-
 321 posite from early in the observation period (AVHRR 6 Mar), and
 322 late (MODIS, 9 Mar). A Lagrangian float was deployed in the
 323 front (black curve), and the ship tracks bracketed the float's posi-
 324 tion (green: *R/V Atlantis*, magenta: *R/V Knorr*). *R/V Atlantis*
 325 cross-sections labeled a-d are shown in Fig. 2a-d.
 326
 2 **Cross sections of data collected across the Gulf Stream.**
 327 Y is the cross-stream distance perpendicular to the path of the
 328 float, positive being northwards. The four columns correspond
 329 to the four sections labeled a-d in Fig. 1. Potential density is
 330 contoured in black and $\sigma_\theta = 26.25 \text{ kg m}^{-3}$ is magenta. Along a
 331 constant density surface salty water is warmer than fresher water,
 332 so the GS on the left is warm and salty. Section a) is the fur-
 333 thest upstream section (65W) and d) is the furthest downstream
 334 (63.75 W) (Fig. 3b). e)-h) downstream velocity calculated rela-
 335 tive to the float's trajectory by removing the float's mean speed
 336 of $u_{\text{float}} = 1.4 \text{ m s}^{-1}$ for the observation period. Green contours
 337 are regions in temperature-salinity space labeled "streamers" in
 338 Fig. 3a. i)-l) Potential vorticity sections (see textmethods); . . .
 339
 14

- 340 3 Streamer properties and distribution in space. a) Loga-
 341 rithmically scaled histogram in temperature-salinity space (colours).
 342 The warm-salty GS water is ~~very~~-distinct from the water to the
 343 north, which is cold and fresh. The water near the surface is hea-
 344 vily modified by the atmosphere. Deeper, there is a class of water
 345 distinct from the GS water and the water to the north, that we
 346 label “streamers”. This water is contoured in green in Fig. 2e-l.
 347 b) Interpolation of salinity, velocity, and potential vorticity onto
 348 the $\sigma_\theta = 26.25 \text{ kg m}^{-3}$ isopycnal, plotted geographically (with
 349 a small exaggeration of scale in the north-south direction, and
 350 the latter two fields offset slightly to the south-east). This used
 351 data from both ships. The ship track for the *Atlantis* is plotted
 352 in black, and the four cross-sections in Fig. 2 are plotted in magenta.
 353 The streamer water is contoured in green. c) The width
 354 of the T/S front attached to the north wall, averaged between
 355 110 and 185 m (green line). The grey line is the width of all the
 356 water in the “streamer” T/S class. A water parcel is considered
 357 “attached” if there there is no more than one kilometer of water
 358 from the fresher water class to the north. This is meant to exclude
 359 the clearly detached streamers. 15

360 4 Evidence for entrainment of intrusions from a dye re-
361 lease and numerical simulation. a) Salinity section from
362 an occupation of the GS 14 March. The location of a dye is
363 contoured in magenta. b) Salinity section from downstream. A
364 streamer has enfolded the dye in cold-fresh water between itself
365 and the GS. c) Temperature-salinity diagram for this occupa-
366 tion. The temperature-salinity for the dye is coloured in dark
367 magenta. d) Salinity in the GS on the $\sigma_\theta = 26.25 \text{ kg m}^{-3}$ isopyc-
368 nals from a high-resolution numerical simulation at t_0 . The green
369 contours delineate the location of particles seeded downstream in
370 the streamer at time $t_1 = t_0 + 70\text{h}$ (see panels e and h) and ad-
371 vected *backwards* in time to t_0 showing where the streamer water
372 originated. The dark magenta contour is the location of particles
373 seeded in the fresh intrusion. The straight line shows the location
374 of the salinity cross-section in panel g. e) as panel d, except at
375 $t_1 = t_0 + 70\text{ h}$; this is the time and locations where the two clouds
376 of particles were seeded. g) and h) salinity cross sections for times
377 t_0 and t_1 . The location of the particles is shown in green and dark
378 magenta contours. The the $\sigma_\theta = 26.25 \text{ kg m}^{-3}$ isopycnal is con-
379 toured in light magenta. These panels show that the origin of the
380 streamer water was in the GS front, and that the fresh-cold water
381 (magenta contour) enfolded against the front came from north of
382 the front. f) shows the speeds of the particle clouds in time, and
383 shows that the intrusion water (magenta) accelerates relative to
384 the streamer water (green). i) The temperature-salinity of all
385 the data at t_1 , with the clouds of seeded particles indicated in
386 T/S space. Note that the green streamer water occupies a mixed
387 mode between the warm GS waters and the cold and fresh water
388 to the north.

Acknowledgements Our thanks to the captains and crews of *R/V Knorr* and *R/V Atlantis*,
390 The AVHRR Oceans Pathfinder SST data were obtained from the Physi-
391 cal Oceanography Distributed Active Archive Center (PO.DAAC) at the
392 NASA Jet Propulsion Laboratory, Pasadena, CA. <http://podaac.jpl.nasa.gov>.
393 Funding was supplied by Office of Naval Research, Grants XXXXXX

Author Contributions JMK did the main analysis of the data and wrote the paper. JMK, CL,
394 EAD, KS, MS, AS, LT collected the data, performed quality control. RH
395 supplied satellite imagery both at sea and on land. JG, JM and JM ran
396 the simulations and analyzed them. All authors contributed significantly
397 to the analysis and interpretation of these results.

Competing Interests The authors declare that they have no competing financial interests.

Correspondence Correspondence and requests for materials should be addressed to Jody
401 M. Klymak. (email: jklymak@uvic.ca).

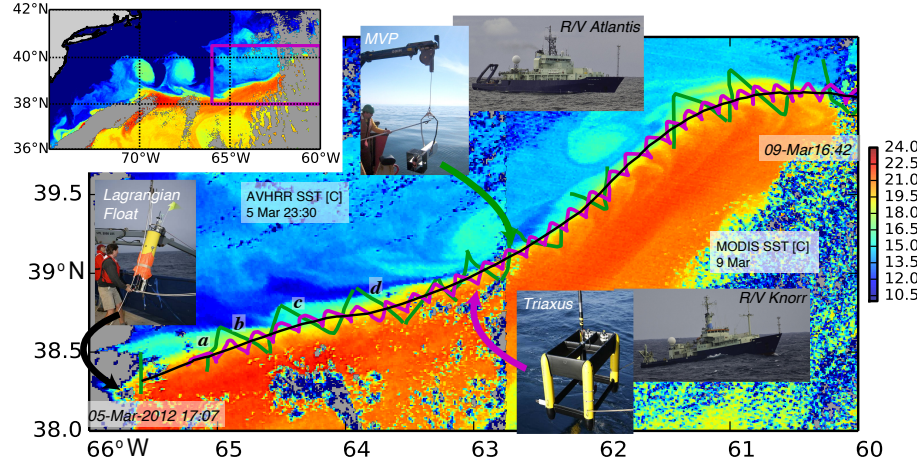


Figure 1: Experimental design. Inset: The experiment site on the north wall of the Gulf Stream, between 66 and 60 W, as shown in an AVHRR satellite image of sea surface temperature (SST). Main: Detailed SST image composed from two ~~satellites~~ satellite images. The GS is warm and delineated by a sharp front. ~~There are~~ The small sub-mesoscale structures north of the front, which are the focus of this paper. The satellite images are a composite from early in the observation period (AVHRR 6 Mar), and late (MODIS, 9 Mar). A Lagrangian float was deployed in the front (black curve), and the ship tracks bracketed the float's position (green: *R/V Atlantis*, magenta: *R/V Knorr*). *R/V Atlantis* cross-sections labeled a-d are shown in Fig. 2a-d.

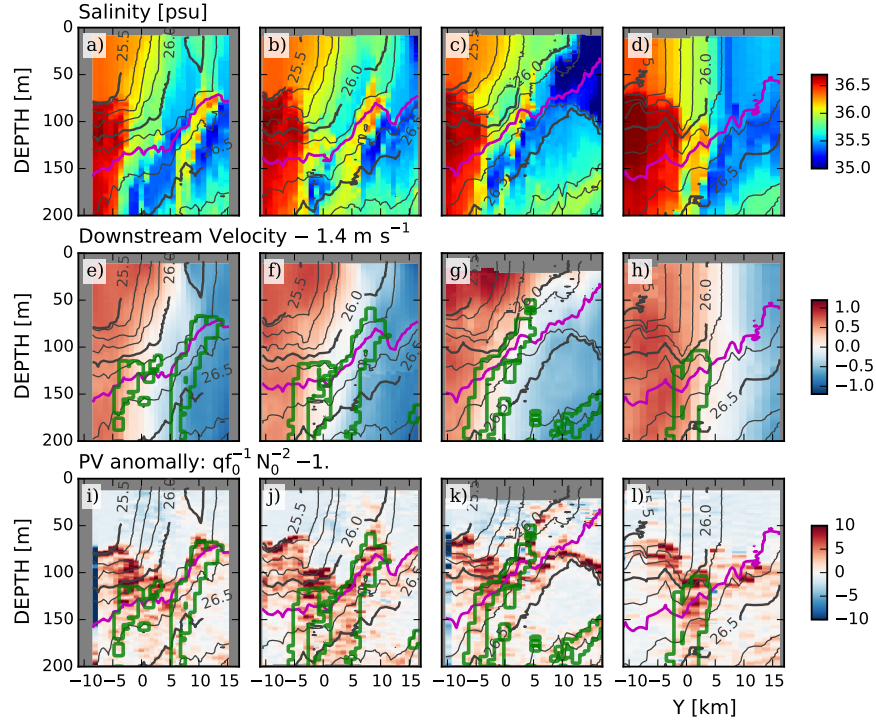


Figure 2: Cross sections of data collected across the Gulf Stream. Y is the cross-stream distance perpendicular to the path of the float, positive being northwards. The four columns correspond to the four sections labeled a-d in Fig. 1. Potential density is contoured in black and $\sigma_\theta = 26.25 \text{ kg m}^{-3}$ is magenta. Along a constant density surface salty water is warmer than fresher water, so the GS on the left is warm and salty. Section a) is the furthest upstream section (65W) and d) is the furthest downstream (63.75 W) (Fig. 3b). e)–h) downstream velocity calculated relative to the float’s trajectory by removing the float’s mean speed of $u_{\text{float}} = 1.4 \text{ m s}^{-1}$ for the observation period. Green contours are regions in temperature-salinity space labeled “streamers” in Fig. 3a. i)–l) Potential vorticity [sections](#) (see [text](#)[methods](#));

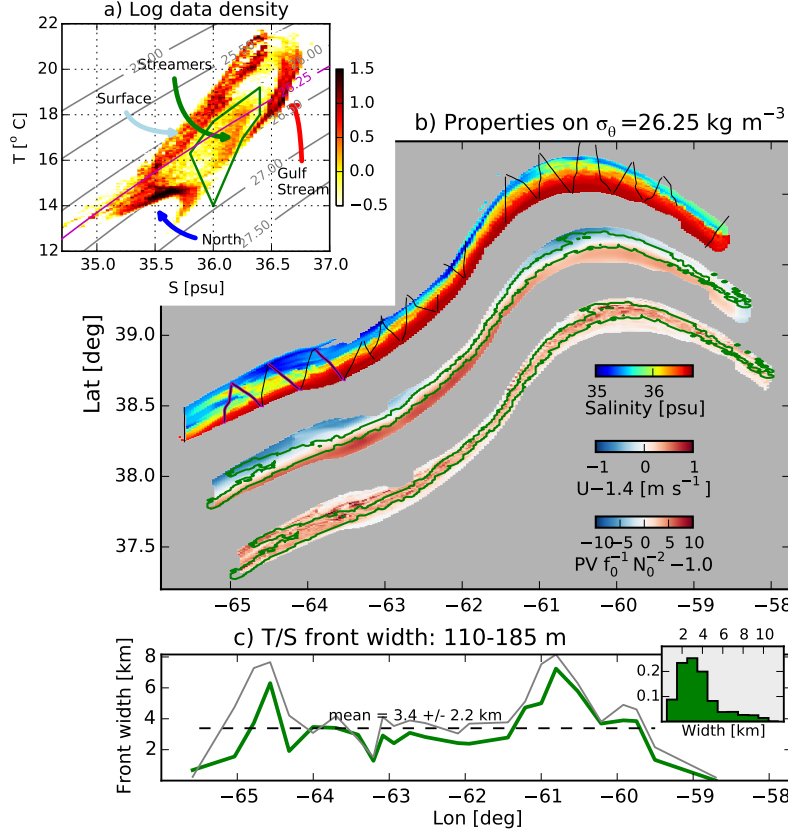


Figure 3: Streamer properties and distribution in space. a) Logarithmically scaled histogram in temperature-salinity space (colours). The warm-salty GS water is very-distinct from the water to the north, which is cold and fresh. The water near the surface is heavily modified by the atmosphere. Deeper, there is a class of water distinct from the GS water and the water to the north, that we label “streamers”. This water is contoured in green in Fig. 2e-l. b) Interpolation of salinity, velocity, and potential vorticity onto the $\sigma_\theta = 26.25 \text{ kg m}^{-3}$ isopycnal, plotted geographically (with a small exaggeration of scale in the north-south direction, and the latter two fields offset slightly to the south-east). This used data from both ships. The ship track for the *Atlantis* is plotted in black, and the four cross-sections in Fig. 2 are plotted in magenta. The streamer water is contoured in green. c) The width of the T/S front attached to the north wall, averaged between 110 and 185 m (green line). The grey line is the width of all the water in the “streamer” T/S class. A water parcel is considered “attached” if there is no more than one kilometer of water from the fresher water class to the north. This is meant to exclude the clearly detached streamers.

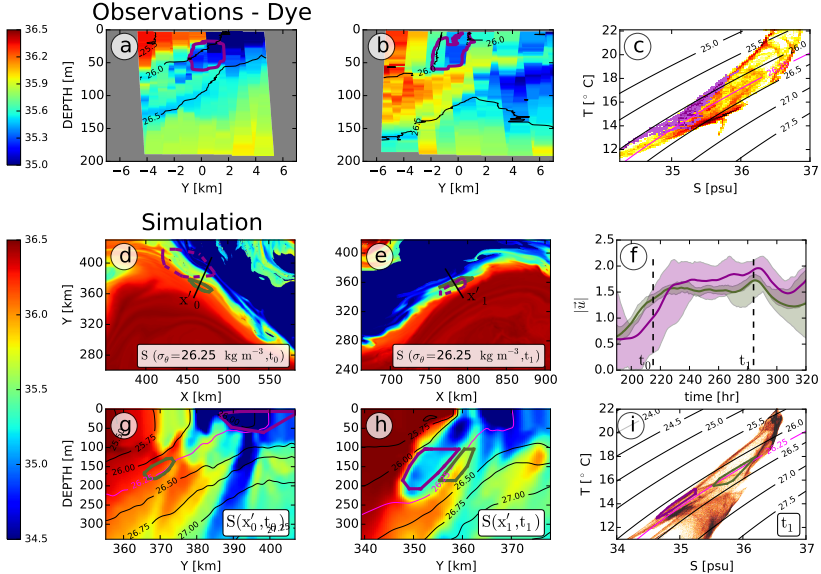


Figure 4: Evidence for entrainment of intrusions from a dye release and numerical simulation. a) Salinity section from an occupation of the GS 14 March. The location of a dye is contoured in magenta. b) Salinity section from downstream. A streamer has enfolded the dye in cold-fresh water between itself and the GS. c) Temperature-salinity diagram for this occupation. The temperature-salinity for the dye is coloured in dark magenta. d) Salinity in the GS on the $\sigma_\theta = 26.25 \text{ kg m}^{-3}$ isopycnal from a high-resolution numerical simulation at t_0 . The green contours delineate the location of particles seeded downstream in the streamer at time $t_1 = t_0 + 70\text{h}$ (see panels e and h) and advected *backwards* in time to t_0 showing where the streamer water originated. The dark magenta contour is the location of particles seeded in the fresh intrusion. The straight line shows the location of the salinity cross-section in panel g. e) as panel d, except at $t_1 = t_0 + 70\text{ h}$; this is the time and locations where the two clouds of particles were seeded. g) and h) salinity cross sections for times t_0 and t_1 . The location of the particles is shown in green and dark magenta contours. The the $\sigma_\theta = 26.25 \text{ kg m}^{-3}$ isopycnal is contoured in light magenta. These panels show that the origin of the streamer water was in the GS front, and that the fresh-cold water (magenta contour) enfolded against the front came from north of the front. f) shows the speeds of the particle clouds in time, and shows that the intrusion water (magenta) accelerates relative to the streamer water (green). i) The temperature-salinity of all the data at t_1 , with the clouds of seeded particles indicated in T/S space. Note that the green streamer water occupies a mixed mode between the warm GS waters and the cold and fresh water to the north.